NMR and Modeling Studies of a Synthetic Extracellular Loop II of the κ Opioid Receptor in a DPC Micelle†

Li Zhang,‡ Robert N. DeHaven,§ and Murray Goodman*,‡

Department of Chemistry and Biochemistry, University of California at San Diego, 6223 Pacific Hall, La Jolla, California 92093-0343, and Adolor Corporation, 371 Phoenixville Pike, Malvern, Pennsylvania 19355

Received September 14, 2001

ABSTRACT: This paper provides the first direct experimental evidence for the secondary structural features of the putative second extracellular loop (ECL II) of the κ opioid receptor through a synthetic peptide mimic in a DPC micelle environment. These studies indicate that residues $V^{6}-A^{15}$ of the ECL II peptide adopt a well-defined helical structure analogous to that formed by $V^{201}-C^{210}$ of the native receptor. Moreover, a β-turn around the D^{22} (D^{217}) and D^{23} (D^{218}) residues represents another feature of the ECL II. The NMR and fluorescent data also suggest the location of the two helical turns of TM V and the approximate location of the C-terminal end of the TM IV of the κ opioid receptor. We modeled the κ opioid receptor including the extracellular region of the receptor. The model of the ECL II utilized the information obtained from the NMR structural analysis of the ECL II peptide in a DPC micelle solution and the molecular dynamic simulations in a biphasic membrane environment. Our discovery of this amphiphilic helical region in the ECL II peptide by NMR and molecular modeling studies provides direct evidence that the sequence of residues $V^{201}-C^{210}$ is likely to be the helical region that interacts with Dynorphin (Dyn) A [Paterlini, G., Portoghese, P. S., and Ferguson, D. M. (1997) *J. Med. Chem. 40*, 3254−3262]. We believe that this work offers further insight into the structural characteristics of the extracellular portions of the seven-TM κ opioid receptor.

Opioids are therapeutic agents for the management of pain, which bind to the opioid receptors mainly distributed in the peripheral and central nervous systems. The κ, μ, and δ subtypes are the three major subtypes of opioid receptors. These receptor subtypes display differential selectivity for opioid ligands, and activation of the receptors leads to diverse clinical effects. It is believed that the binding of opioids to these receptors initiates a descending noceptive control system by inhibiting the ascending pain tracts. In particular, the κ receptor is activated by the endogenous heptadecapeptide Dynorphin (Dyn)[1] A (1−17) (Tyr-Gly-Gly-Phe-Leu^{5}-Arg-Arg-Ile-Arg-Pro^{10}-Lys-Leu-Lys-Trp-Asp^{15}-Asn-Gln-OH).

The κ receptor, as well as the μ and δ receptors, belongs to the superfamily of G-protein-coupled receptors, which are integral membrane proteins presumed to have the common structural motif of seven transmembrane (TM) helices, connecting loops, and long N- and C-terminal tails at the extracellular and intracellular domains. The X-ray structure of the κ receptor has not been determined because of the difficulties in the crystallization of membrane proteins. Investigations with κ opioid receptor chimeras have shown that the putative second extracellular loop (ECL II) contributes substantially to the κ receptor's selectivity in Dynorphin ligand recognition (*1*−*3*). In addition, the ECL II domain contains eight acidic amino acids. Dyn A (1−13), on the other hand, includes five basic amino acids (from Arg^{6} to Lys^{13}). Their removal (*4*, *5*) or substitution by Ala (*6*) causes a marked decrease in κ selectivity, especially in the case of Arg^{7}. While residues 12−17 in Dyn A (1−17) can be truncated without a significant loss in bioactivity (*7*), it is reasonable to speculate that Dyn A binds to the κ receptor through Coulombic interactions. However, other investigators, such as Paterlini and Ferguson et al. (*8*), performed docking studies based on a homology model of the κ receptor and have proposed that a helical domain of the ECL II interacts with Dyn A (1−10) through hydrophobic interactions.

Unfortunately, the structural data of the κ receptor are limited to theoretical models, because experimental techniques such as NMR and X-ray analysis are not currently generally applicable to transmembrane receptors. To unveil the mechanism of activation and selection of the κ receptor to its ligands, it is crucial to study the structural features of the ECL II of the κ receptor under biologically relevant conditions. An understanding of the molecular mechanism by which these Dynorphin ligands interact with and activate the κ receptor is an important step toward the development of novel drugs that have the potential to induce analgesia

† This work is supported by NIHDA Grant 05539.

* To whom correspondence should be addressed.

‡ University of California at San Diego.

§ Adolor Corp.

[1] Abbreviations: ECL II, second extracellular loop; Dyn, Dynorphin; TM, transmembrane; DPC, dodecylphosphocholine; FMOC, fluorenylmethoxycarbonyl; *t*Bu, *tert*-butyl; Trt, trityl; Boc, *tert*-butyloxycarbonyl; DMF, dimethylformamide; DIPEA, diisopropylethylamine; HATU, *O*-(7-azabenzotriazol-1-yl)-1,1,3,3-tetramethyluronium hexafluorophosphate; HFIP, hexafluoro-2-propanol; CD, circular dichroism; DMPC, dimyristoylphosphatidylcholine; DHPC, dihexanoylphosphatidylcholine; MD, molecular dynamics; CCl_4, carbon tetrachloride.

10.1021/bi0117955 CCC: $22.00
Published on Web 12/05/2001

without causing the respiratory depression or addiction associated with μ opioid receptor agonists such as morphine (*9*).

Recent work by Yeagle et al. on rhodopsin suggested that it is feasible to elucidate the structures of the G-protein-coupled receptors by piecing together the structural domains (*10*, *11*). Furthermore, Yeagle et al. successfully demonstrated that the loops of rhodopsin are stabilized by short-range interactions, which are determined by the amino acid sequence (*11*, *12*). A number of NMR studies of linear peptides, corresponding to the natural sequence of the intra- and extracellular loops and termini of the receptors, were reported by Yeagle et al. (*13*−*17*), Mierke et al. (*18*−*22*), and others (*23*−*25*). Thus, well-designed synthetic fragments of a receptor should be able not only to provide a reliable method for identification of the structural features of the loops but also to define the entry points of the loops at the TM domains of the receptors (*22*).

Dodecylphosphocholine (DPC) micelles often are chosen as "membrane mimics" for studying peptide−membrane interactions by using high-resolution NMR techniques. The zwitterionic phosphatidylcholine headgroup of DPC is similar to that found in biological membranes. Like SDS, DPC forms small micelles of 50−60 molecules that rapidly reorient in solution (*26*). The micelles are stable over a wide range of temperatures and pHs, which is important for NMR investigations.

To explore the structural features contributing to the specific binding of the ECL II of the κ receptor to its selective analogues, we synthesized a 33-amino acid peptide composed of the sequence (residues 196−228) based on the ECL II sequence of the human κ opioid receptor. In addition to the amino acid residues believed to constitute the ECL II of the receptor, this peptide included N-terminal and C-terminal amino acids believed to reside, respectively, in the transmembrane IV and transmembrane V domains of the κ receptor. C^{210} in the ECL II was replaced with A^{210}, to increase the stability of the synthetic peptide. In addition, the N-terminus was acetylated and the C-terminus amidated. The sequence is Ac-^{196}LGGTKVREDVDVIEASLQFPD-DDYSWWDLFMKI^{228}-NH_2.

MATERIALS AND METHODS

Synthesis and Purification. The synthesis of the ECL II peptide was carried out on a Milligen 9050 peptide synthesizer on a 0.2 mmol scale by the Fmoc solid phase method. All amino acids were free carboxylic acids with FMOC (fluorenylmethoxycarbonyl) protection on the amine. Side chains were protected using *t*Bu (*tert*-butyl) ethers for Ser, Thr, and Tyr; *t*Bu esters for Asp and Glu; Pbf (2,2,4,6,7-pentamethyldihydrobenzofuran-5-sulfonyl) for Arg; Trt (trityl) for Gln; and Boc (*tert*-butyloxycarbonyl) for Lys and Trp (Novabiochem, San Diego, CA). The Fmoc-PAL-PEG-PS resin (PerSeptive Biosystems, Hamburg, Germany) was used as the solid support. The Fmoc amino acids were dissolved in DMF (dimethylformamide) and DIPEA (diisopropylethylamine). All coupling reactions were carried out using the coupling agent HATU, *O*-(7-azabenzotriazol-1-yl)-1,1,3,3-tetramethyluronium hexafluorophosphate (Perseptive Biosystems, Warrington, England), at 50 °C with a coupling time of 1 h. After coupling of all amino acids, the amino terminus was acetylated using a solution of dimethylformamide (87%), dichloromethane (10%), acetic anhydride (3%), and hydroxyazabenzotriazole (12.2 g). The resin was then washed with dichloromethane and dried overnight under vacuum. Cleavage and deprotection were carried out using reagent R (90% TFA, 5% thioanisole, 3% ethanedithiol, and 2% anisole) for 4 h on the shaker. The peptide was cleaved from the resin to yield a carboxyamide terminus. The slurry was filtered through a 30 cm^3 syringe packed with glass wool in the front into a 50 mL centrifuge tube. The filtered solution was then pipetted into a 500 mL cold diethyl ether solution and stored overnight at −20 °C. The precipitate of the crude material that was obtained was collected on a sintered glass funnel, dissolved in HFIP (hexafluoro-2-propanol), and lyophilized to give an off-white powder.

The peptide was not purified by conventional RP-HPLC because it did not dissolve well in the available organic or aqueous phase solvents that were used for RP-HPLC. After many attempts, the loop peptide dissolved in 70% formic acid in a monomeric form without degradation. Thus, the Superdex Peptide HR 10/30 column (Pharmacia Biotech Products, Piscataway, NY) was used for the purification of the loop peptide. The column molecular weight fraction range (M_r) was from 100 to 7000. The matrix was spherical and composed of cross-linked agarose and dextran, with an average particle size of 13 μm. The purification was carried out at a flow rate of 0.4 mL/min to avoid exceeding the 220 psi maximum pressure of the column. An isotropic 70% formic acid elution was carried out on an M-6000 Waters Associates (Milford, MA) chromatography pump with an injection volume of 250 μL at a concentration of 15 mg/mL. UV detection at 280 nm was used throughout. The main elution peak occurred at 21.26 min. The purified peptide was lyophilized with diluted formic acid and then washed with acetone to remove the formic acid. The washed product was redissolved in 500 mM ammonium bicarbonate (pH 8.4) and relyophilized to yield a white powder without aggregation. The identity of the peptide was verified by mass spectrometry and NMR, and was shown to have a purity level of >95%. The monoisotopic mass is 3927.90, and the average mass is 3930.44 (MALDI mass spectrometry).

CD and Fluorescence Experiments. Circular dichroism (CD) spectra were obtained on a Cray 61 spectrometer at 20 °C for the ECL II peptide in four different solvents: DPC micelle, DMPC/DHPC bicelle (*27*) (where [DMPC]/[DPHC] = 0.5), HFIP, and an aqueous solution with phosphate buffer (pH 6.8) (DMPC and DHPC denote dimyristoylphosphatidylcholine and dihexanoylphosphatidylcholine, respectively). The mean residue ellipticity was calculated using a mean molar mass of 3930.44/33 (119.10 g/mol per residue).

A Perkin-Elmer LS50B luminescence spectrometer (Perkin-Elmer, Norwalk, CT) with an attached temperature control unit was used for the fluorescence measurements. All fluorescence spectroscopy experiments were conducted at room temperature in a 2 mL fluorescence cuvette. The concentration of the peptide in the DPC micelle sample was 12.5 μM. Fluorescence emission measurements were carried out by exciting the sample at 280 nm and monitoring emission from 280 to 600 nm. Fluorescence excitation measurements were taken by exciting irradiation from 200

to 340 nm and monitoring at 341 and 352 nm. The spectra of the solvents were subtracted from the sample spectra.

NMR Experiments. The NMR experiments were carried out on both Bruker DRX600 and AMX500 spectrometers. The solutions of the ECL II peptide were prepared at concentrations of 0.5−2 mM. The final concentration of the peptide for two-dimensional experiments was 1.9 mM with 144 mM dodecylphosphocholine-d_{38} (DPC-d_{38}, Avanti Polar Lipids Inc., Alabaster, AL) and 50 mM phosphate buffer at pH 6.8 [1:9 D_2O/H_2O (v/v)]. A 0.29 mM TSP-d_4 (Isotec Inc., Miamisburg, OH) solution was added as an internal standard. The DPC-d_{38} micelle solution was first prepared, followed by addition of the peptide, vortexing, and a short sonication to ensure the homogeneity of the micelle solution. The micellar solutions prepared under these conditions were stable over the time of these experiments, which required approximately 3 months. Between the measurements, the samples were stored at −20 °C. The samples were also prepared in pure D_2O to avoid interference from the H_2O signal to obtain the full assignments of the proton spectra. The spectrum of the sample with H_2O and DPC-d_{38} was acquired with a Bruker 600 MHz spectrometer equipped with a 5 mm TXI (H/C/N-D) triple-resonance probe and three-dimensional field gradients. The water suppression was carried out using a 3-9-19 watergate-pulse sequence (*28*, *29*). The NOESY experiments were performed at mixing times of 100, 200, and 270 ms at temperatures of 288, 298, 310, and 325 K for each mixing time. The TOCSY experiments were performed at mixing times of 30, 50, and 70 ms at the four temperatures given above to obtain the full assignments of the proton spectra. The NMR data were processed on an SGI O2 workstation with Felix98 software. In all the experiments, there were 4K data points collected for the directly detected dimensions and 400−512 data points collected for the indirectly detected dimensions. Sinbell 60° shift or Sinbell 90° shift window functions were applied for both dimensions before data processing for TOCSY, DQF-COSY, NOESY, and ROESY. The second dimension was zero filled to the same number of data points as the first dimension, and baseline correction was applied to the second dimension. All the proton chemical shifts were referenced relative to the internal standard TSP-d_4 (0 ppm).

The ^1H homonuclear NMR experiments for the sample in a D_2O/DPC-d_{38} solution were carried out with a Bruker 500 MHz spectrometer equipped with a 5 mm TXI (H/C/N-D) triple-resonance probe. The D_2O/DPC-d_{38} sample was prepared after lyophilizing the sample in an H_2O/DPC-d_{38} solution, and then equilibrated with pure D_2O. The residual water resonance was suppressed by direct irradiation (1 s) at the water frequency during the relaxation delay between scans for TOCSY and DQF-COSY experiments and also during the mixing time in NOESY experiments.

Molecular Modeling. Conformations of the ECL II peptide were calculated using the DGII method (*30*) (Molecular Simulations Inc., San Diego, CA). The DGII protocol starts with bound smoothing, in which a triangular inequality strategy is applied, followed by random metrization (i.e., converting the distance matrix into a centroidal metric matrix) with the coordinates and appropriate distances obtained by angular embedding and majorization procedures (i.e., improving the least-squares fit of these coordinates to the distance matrix). The DG structures were optimized by simulated annealing and conjugate gradient minimization. Distance restraints derived from the NOE intensities were divided into strong (<2.5 Å), medium (2.5−3.5 Å), and weak (3.5−5.0 Å) boundary conditions. The cross-peaks that are close to the diagonal and overlapped peaks are only used for the qualitative estimation for the calculation. The DGII calculations, starting with an extended linear chain of the ECL II peptide (residues 1−33 or 196−228), resulted in a cluster of structures satisfying restraints derived from NMR spectra.

The family of structures deduced from the NOE restraints displays common secondary structural features, but the experimental data do not allow the determination of the relative topological arrangement of the peptide termini. We carried out an explicit solvent simulation to determine the topological orientation and the depth of insertion of the ECL II peptide with the anisotropic, biphasic environment.

Kessler et al. applied an H_2O/CCl_4 mixture as a membrane mimetic during molecular dynamics (MD) to reproduce both the proper orientation of the amphiphilic and correct phase preference of lipophilic organic molecules (*31*). Therefore, we have taken one of the representative lowest-energy conformations derived from NMR distant restraints for extensive MD simulations in a CCl_4/H_2O biphasic box. During the MD simulations, the two ends of the loop peptide were fixed to the same distance as that between TM IV and TM V within the κ receptor at the beginning of the simulation.

The CHARMm program (Molecular Simulations Inc.) was used for all the subsequent minimizations and MD simulations. A periodical boundary condition was applied in both minimization and MD simulations. The long-range forces were handled by using a 14 Å nonbonded cutoff and a switching function. Shake restraints were applied to the bonds containing hydrogen so that a 0.002 ps time step could be used.

Separately equilibrated water and carbon tetrachloride (CCl_4) boxes were used for the construction of the biphasic cell. The ECL II peptide was placed in the simulation cell with the center of the peptide in the origin of the biphasic cell and several different initial positions. The L^1−K^5 sequence at the N-terminal end and the W^{27}−I^{33} sequence at the C-terminal end were modeled as TM helices. CCl_4 and H_2O of the solvent were deleted if they were within 2.8 Å of the heavy atoms of the ECL II peptide. One thousand steps of steepest descent minimization were performed initially with convergence of 1 kcal/mol. If 30 ps of heating and equilibration is not included, a total of 1 ns of MD simulation was carried out for the ECL II peptide in the biphasic box. The interface and ECL II peptide were stable during the 1 ns MD simulations. The simulations of the ECL II peptide in an explicit H_2O/CCl_4 solvent box have allowed for the classification of a diverse range of peptide−biphasic solvent interactions.

The model building of the extracellular phase and TM domain of the κ receptor involves a combination of structural homology modeling and incorporation of the final conformation of the ECL II peptide in the biphasic box (for details, see the Supporting Information). We built TM regions of the κ receptor based on the recently published X-ray structure

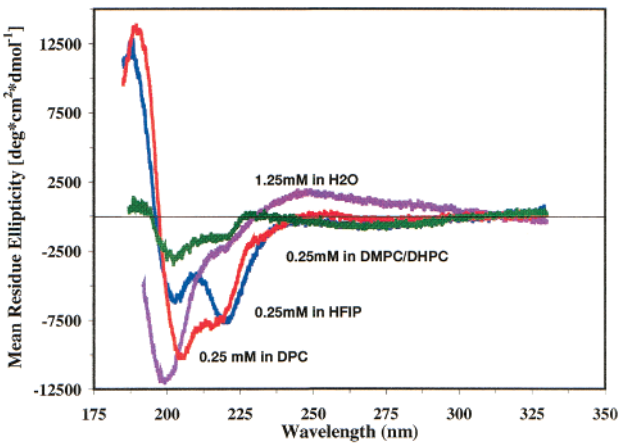

FIGURE 1: CD spectrum of the ECL II peptide in various solvents at 20 °C. The ECL II peptide exhibits helical secondary structure in various membrane mimetics and HFIP, while the structure in aqueous solution is random.

of rhodopsin (1F88) (*32*). The ECL I and ECL III of the κ receptor were modeled from a database search since they are both short in length, four and nine residues, respectively. The refined ECL II structure was manually docked to the transmembrane domain by superposition of the overlapping portions of TM IV and TM V. Because there is a disulfide bridge between C^{131} at the top of TM III and C^{210} (A^{210}) in the ECL II, the $\alpha-\alpha$ distance between these two residues was used as a restraint for the further MD and energy minimization of the modeling structure.

RESULTS AND DISCUSSION

CD and Fluorescence Studies. We utilized a sequence prediction algorithm (*33*) that predicted a high helical propensity in the V^{12}IEASLQ^{18} and W^{26}WDLFMKI^{33} sequences of the ECL II peptide. A useful start to the structural analysis involves the use of CD to obtain a measure of the overall secondary structural content of the peptide. The CD measurement of the ECL II peptide was carried out in organic and aqueous solutions and in membrane mimetic bicelles and micelles. As shown in Figure 1, the ECL II peptide exhibits different degrees of helicity in a DPC micelle, a DMPC/DHPC bicelle, and HFIP solvents, with characteristic double minima in the CD spectra at 222 and 208 nm. In contrast, the ECL II peptide is disordered in an aqueous medium. This demonstrates that the selection of the solvent for the structural determination is critical, especially for membrane proteins. We believe that DPC is a good choice of solvent for carrying out the NMR studies for the partially membrane-embedded ECL II peptide.

By inspecting the sequence of the ECL II peptide, we found that the two tryptophans at the C-terminus should provide information about the interaction of the ECL II peptide with the DPC micelle. Therefore, we carried out steady-state fluorescence studies with the ECL II peptide both in an aqueous medium and in the DPC micelle medium. In aqueous solution, there is one emission peak at 356 nm. In the DPC micelle solution, there is a very broad emission peak from 341 to 352 nm (Figure 2). The broad peak results from two equal populations of two overlapping tryptophan peaks of the ECL II peptide, which are too close to be separated. According to studies by Deber et al. (*34*), the blue shifts of the Trp emission peaks demonstrate the effect of the hydrophobic environment of the micelle, indicating that the two Trp residues of the ECL II peptide were at the interface of the DPC micelle and H_2O solvent.

NMR Data and Secondary Structural Features. The NMR spectral assignments followed the basic principles from the standard homonuclear NMR methods (*35*). Most of the spectral overlap occurred in the H$\alpha-$NH region, which was overcome by comparing data at different temperatures and spectra acquired with only a DPC/D_2O solution. Dispersion of the Hα and Hβ cross-peaks facilitated the assignment of the resonance in the TOCSY and NOESY spectra. The complete assignments for the ECL II peptide are summarized in Table 1 (Supporting Information). The line widths were too broad for these spectra taken in the DPC micelle to analyze the coupling constants adequately.

The secondary shifts for Hα were calculated by subtracting the Hα chemical shifts for the unstructured peptide (*36*, *37*)

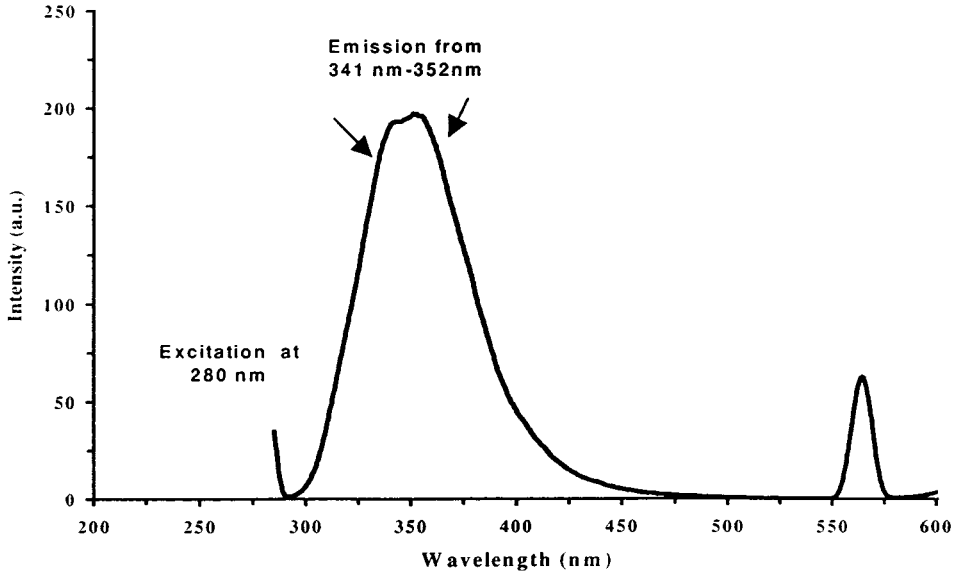

FIGURE 2: Steady-state fluorescence excitation and emission spectrum of the ECL II peptide in DPC. One of the Trp residues is blue-shifted from 352 to 341 nm. This indicates that it interacts with the hydrophobic interior of the DPC micelle.

Table 1: Torsional Angles (rmsds) for the Backbone of the Loop Peptide in Degrees

	Leu[1]	Gly[2]	Gly[3]	Thr[4]	Lys[5]	Val[6]	Arg[7]	Glu[8]	Asp[9]	Val[10]	Asp[11]	Val[12]	Ile[13]
ϕ	−	−168 (87)	−125 (55)	−106 (38)	−53 (4)	−58 (3)	−66 (8)	−57 (2)	−61 (2)	−62 (1)	−66 (6)	−61 (3)	−64 (1)
ψ	−20 (90)	−49 (89)	41 (76)	105 (7)	−47 (4)	−49 (4)	−46 (4)	−53 (3)	−45 (3)	−48 (2)	−48 (5)	−46 (2)	−53 (5)
ω	179 (2)	178 (2)	−179 (1)	−177 (1)	176 (1)	176 (0)	176 (2)	176 (1)	176 (1)	176 (1)	177 (2)	176 (1)	177 (1)

	Glu[14]	Ala[15]	Ser[16]	Leu[17]	Gln[18]	Phe[19]	Pro[20]	Asp[21]	Asp[22]	Asp[23]	Tyr[24]	Ser[25]	Trp[26]
ϕ	−57 (5)	−84 (6)	−119 (20)	−103 (18)	−86 (17)	−118 (14)	−67 (9)	−63 (3)	−75 (5)	−100 (28)	22 (65)	−74 (2)	−90 (21)
ψ	−47 (2)	−19 (14)	−64 (16)	54 (39)	89 (8)	96 (13)	164 (4)	−53 (4)	−45 (25)	−3 (65)	−60 (9)	71 (14)	−56 (14)
ω	178 (1)	−179 (1)	−178 (1)	−179 (1)	−179 (2)	−178 (1)	179 (1)	178 (0)	179 (1)	−177 (2)	179 (1)	179 (1)	178 (2)

	Trp[27]	Asp[28]	Leu[29]	Phe[30]	Met[31]	Lys[32]	Ile[33]
ϕ	−77 (12)	−69 (11)	−72 (8)	−55 (4)	−64 (7)	−75 (22)	−82 (14)
ψ	60 (46)	−54 (7)	−42 (6)	−53 (4)	−30 (21)	−47 (5)	−39 (1)
ω	179 (2)	175 (1)	178 (1)	175 (0)	176 (1)	178 (0)	−

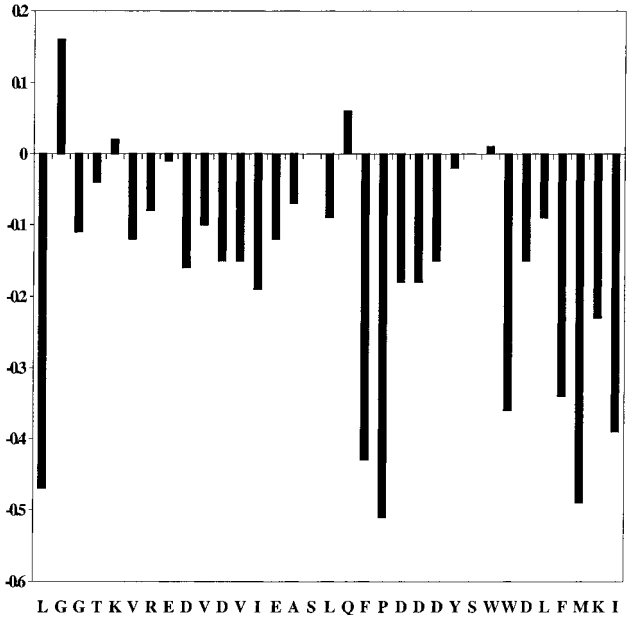

FIGURE 3: Differences in the Hα secondary chemical shifts observed and those reported for unstructured peptides for the ECL II peptide in DPC-d_{38} (the chemical shifts of the Hα's of S[16] and S[25] cannot be unambiguously assigned).

from the experimentally measured Hα chemical shifts of the ECL II peptide. The consecutively negative values observed for V[6]−A[15] and W[26]−I[33] (Figure 3) suggest the presence of α-helical structure in these two regions (*36*). The relevant backbone NOEs are presented in Figure 4. As shown in Figure 4, the $H^N-H^N(i, i+1)$ NOEs for the ECL II peptide reside in two main peptide segments: V[6]−A[15] and W[26]−I[33]. There is also a contiguous stretch of medium-range $\alpha N(i, i+3)$ and $\alpha\beta(i, i+3)$ NOEs within the V[6]−A[15] region. These data support the presence of a predominantly α-helical structure within the V[6]−A[15] region. On the other hand, at the C-terminus of the ECL II peptide, there are few $i, i+3$ NOEs, which are indicative of two turns of a nascent α-helix (*38*), which are present for only a small percentage of the ensemble of structures or for only a short period of time. In addition, the $H^N-H^N(i, i+1)$ and $H^\alpha-H^N(i, i+1)$ NOEs between D[22] and D[23], and between D[23] and Y[24], indicate a tight β-turn about the D[22] and D[23] residues.

The NOESY spectra (Figure 5a,b) in the NH region at both 310 and 298 K display a series of correlations of the H^N_i to H^N_{i+1} type. In contrast, the NH−NH NOEs from V[6] to E[8] appear at 298 K and not at 310 K. This indicates that the helix segment of residues V[6]−Ala[15] unwinds partially from the N-terminal end at elevated temperatures or is more flexible at higher temperatures. In addition, both spectra exhibit obvious line broadening for the C-terminal residues compared with residues from the V[6]−A[15] sequence. This suggests that C-terminal residues are in a different environment (DPC membrane) than the residues from the V[6]−A[15] sequence and the rest of the ECL II peptide.

The interaction between the ECL II peptide and the DPC micelle plays an important role in the conformation of the peptide. Fluorescence and NMR data suggest that starting from W[221] or W[222] approximately seven residues at the

FIGURE 4: Relevant NOEs detected from NOESY spectra at 298 and 310 K and utilized in the structure calculations. A shaded bar indicates a cross-peak not unambiguously identified due to resonance overlap.

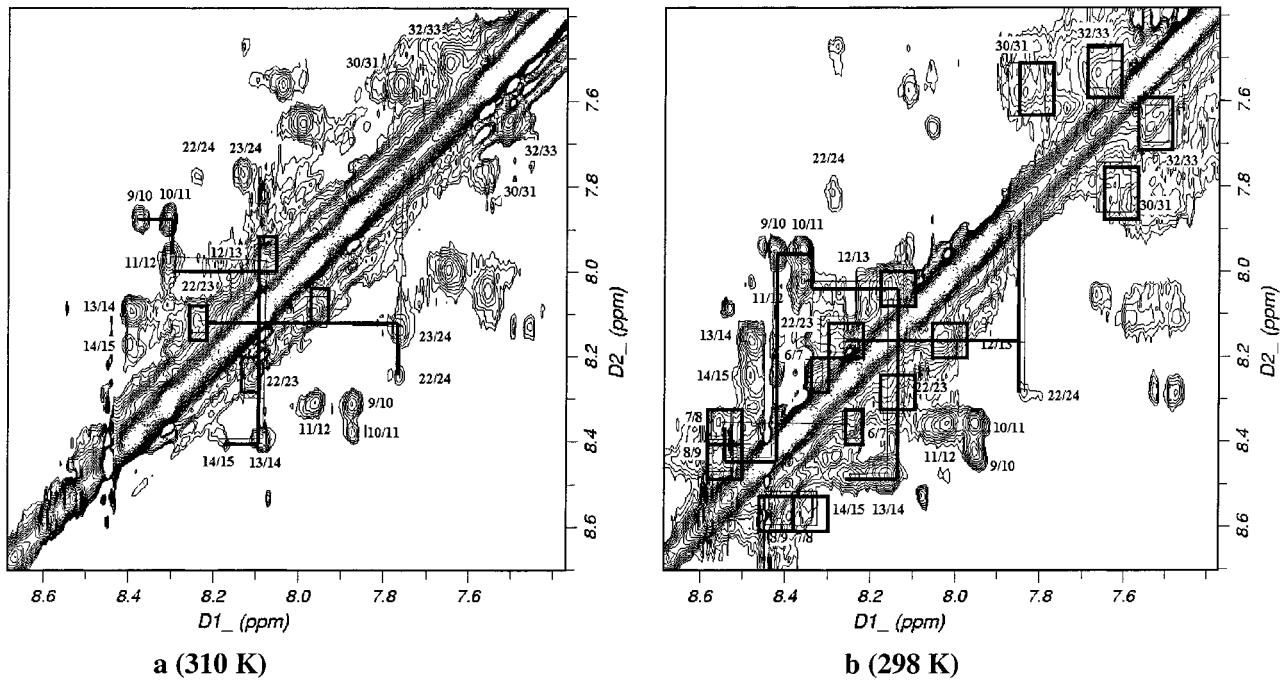

FIGURE 5: Sequential NH−NH NOEs indicate the helical region from V^{201} to A^{210} (residues 6−15) and nascent helix at the C-terminus for the ECL II peptide (residues are labeled as the sequential numbers in the peptide sequence) at 310 (a) and 298 K (b).

C-terminus were inserted into the DPC membrane mimetics. Evidence also indicates that the N-terminal residues, L^1−K^5, are partially embedded in the DPC micelle. (1) L^1 interacts closely with the DPC micelles, supported by the diminishing TOCSY transfer of the side chain for L^1. (2) R^7 at the N-terminus most likely interacts with the phosphatidylcholine headgroups, which is demonstrated by the equivalent line broadening of the side chains of R^7 and K^{32} as compared to that of K^5.

The final refined structures (Figure 6) deduced from DG and simulated annealing present a family of structures that display a helical array from V^6 to A^{15} with an rmsd of 0.48 Å for the backbone atoms. The peptide is relatively undefined in the middle hinge region, because the S^{16}−P^{20} sequence yields few NOEs. Following D^{21} is a β-turn spanning three consecutive Asp residues (D^{21}−D^{23}) and Y^{24}. The C-terminus of the peptide displays a helical turn tendency. Additionally, the residues following V^6 form a turn of approximately 90° from the N-terminus to accommodate the strong NOE between the NH group of R^7 and methyl group of T^4. The rmsds of the backbone torsional angles for the ECL II peptide are reported in Table 1 for a cluster of 14 structures (Figure 6) to demonstrate the divergence of the structures and relative refinement of the different parts of the ECL II peptide.

Extracellular Loop II and the κ Receptor. The inclusion of a greater number of residues in the ECL II peptide in constituting the C-terminal end of TM IV may lead to creation of a stable and better anchored hydrophobic helix. However, the MD simulations in the biphasic box incorporating the distance restraints at the two ends of the ECL II peptide in the initial stage of the simulations suggest a global orientation with both termini projecting into the lipid environment.

The final conformation of the ECL II peptide in the biphasic box that satisfied NOE restraints is shown in Figure 7. Despite the initial placement of the ECL II peptide at the

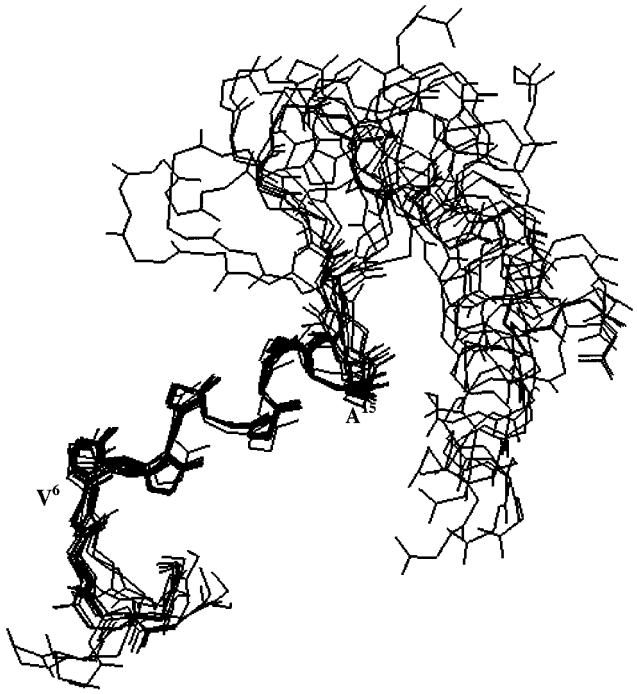

FIGURE 6: Family of the final NMR structures derived from NOE distance restraints displaying the secondary structure feature of the ECL II peptide.

interface, the insertion points at the hydrophobic CCl_4 phase are residues K^5 at the N-terminus and W^{26} and W^{27} at the C-terminus. The amphiphilic character of the helix of residues V^6−A^{15} was demonstrated by the side chains of residues V^6, V^{10}, V^{12}, and I^{13} inserting into the hydrophobic CCl_4 phase. The other interactions of the peptide with CCl_4 are mainly through the hydrophobic interaction of the side chains of L^1 and W^{27}−I^{33}.

The studies by Yeagle et al. on the loop structures of rhodopsin agreed with those by Dyson and Wright et al., who demonstrated that local secondary structure resulted

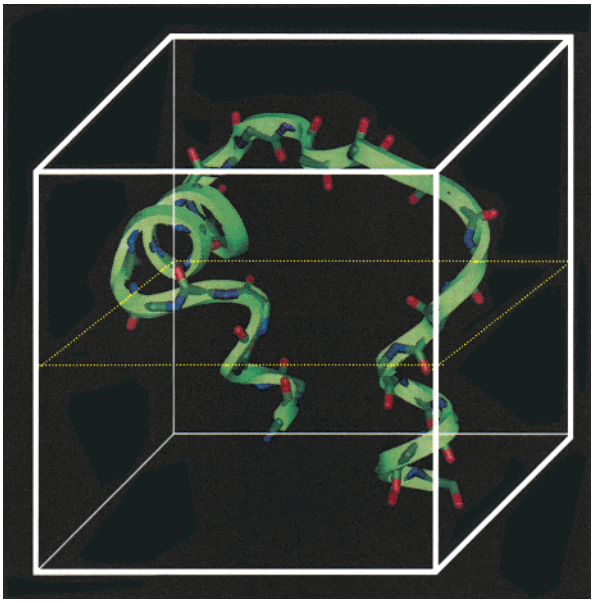

FIGURE 7: Final structure of the ECL II peptide of the κ opioid receptor in CCl_4/H_2O solutions.

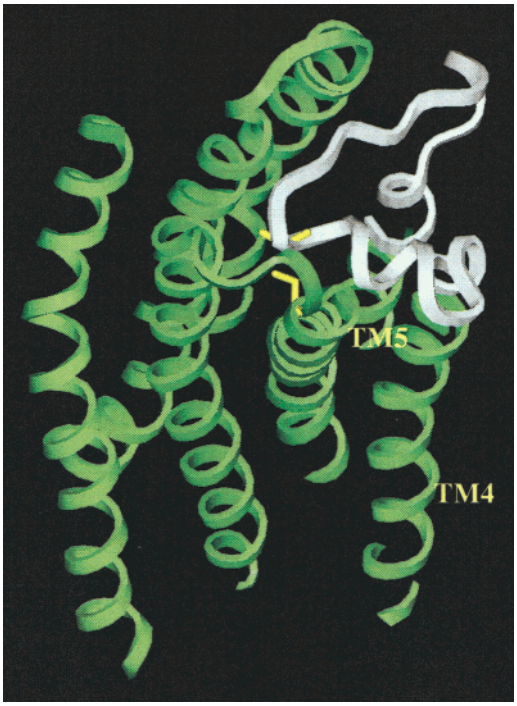

FIGURE 8: Homology model of the κ receptor with an extracellular phase, including the extracellular loop II (ECL II) and short loops of the ECL I and ECL III. The heavy atoms of Cys^{113} and Ala $(Cys)^{210}$ are in yellow.

from short-range interactions and was dictated by the amino acid sequences (*11*, *12*, *38*). Taking advantage of the secondary structural features which were deduced from our NMR studies, we incorporated extra sets of restraints to mimic the native folding of the extracellular loop II to build a model of the ECL II with the receptor (ECL I and ECL III also included) and membrane environment. This model suggests that the ECL II covers the receptor in a liplike manner and the tip of the lip reaches over to the ECL I because of the restraints of a disulfide bridge between C^{131} and C^{210} (A^{210}). The amphiphilic helical region of the ECL II is close to TM III and the ECL I (Figure 8).

CONCLUSIONS

It was the principal objective of this research to provide direct experimental evidence for the secondary structural features of the ECL II (residues 196−228 or 1−33 in the ECL II peptide) of the κ opioid receptor through a synthetic peptide mimic in a micelle environment. We have determined the two helical turns of TM V and the approximate location of the C-terminal end of TM IV of the κ opioid receptor. The linear peptide did not completely mimic the conformation of the ECL II within the receptor, because the N-terminus of the peptide was too short to serve as a helical membrane-tethering point. Nevertheless, we were able to build a model of the extracellular phase of the κ opioid receptor, including the ECL II of the κ opioid receptor based on the secondary structural features determined by the NMR results, homology modeling, and extensive biphasic solvent box simulations.

The binding profile of the κ opioid receptor is relatively unique among the opioid receptors, while those of the μ and δ receptors are similar to each other (*1*). Our results show that the ECL II of the κ receptor displays an amphiphilic helical region from V^{201} to A^{210} (C^{210} in the original sequence), which is not present in the μ and δ receptors. It supports the idea that an amphiphilic helical domain of the ECL II interacts with Dyn A (1−10), a model previously proposed by Paterlini, Ferguson, and co-workers based on sequence analysis and homology modeling of the κ opioid receptor (*8*). In light of the existence of an amphiphilic helical region in Dyn A (1−17) from residue Gly^3 to Arg^9, which was previously studied by Kallick et al. in a DPC micelle environment (*39*), the complementary helix−helix binding mode is a reasonable proposal for the binding of endogenous Dynorphin (*8*). Moreover, the helix−helix interaction is proposed to be hydrophobic in character because the binding of Dyn A (1−13) is essentially not affected by charge neutralization of the ECL II (*40*).

A β-turn around the D^{22} (D^{217}) and D^{23} (D^{218}) residues represents another feature of the ECL II. The side chains of these two aspartic acids are exposed to the aqueous medium. The significance of this β-turn in the ECL II of the κ opioid receptor cannot be determined from our studies.

It was proposed by Schwyzer in 1992 (*41*) that membrane environment plays an important role in ligand binding (*42*). Our results demonstrate the importance of the membrane mimetic environment for studying the conformation of the synthetic ECL II peptide. The secondary structural features of the ECL II of the κ receptor deduced from NMR studies provide experimental evidence for the proposal of a mechanism for association and activation of the κ opioid receptor to its peptide ligand (*8*). Our findings based on the implications provide insights into discoveries using other G-protein-coupled receptors.

ACKNOWLEDGMENT

We thank Prof. Charles Deber (University of Toronto, Toronto, ON) for his helpful discussions. Special thanks are due to Joseph Taulane for his aid with the CD spectrometer. We also express our gratitude to Professor Elizabeth A. Komives for the use of the Milligen 9050 peptide synthesizer. Finally, M.G. is indebted to Kerney J. Glover for his help

in the synthesis and fluorescence studies in a bicelle solution of the loop peptide.

SUPPORTING INFORMATION AVAILABLE

Resonance assignments and structural and modeling data. This material is available free of charge via the Internet at http://pubs.acs.org.

REFERENCES

1. Meng, F., Hoversten, M. T., Thompson, R. C., Taylor, L., Watson, S. J., and Akil, H. (1995) *J. Biol. Chem. 270*, 12730−12736.
2. Xue, J. C., Chen, C. G., Zhu, J. M., Kunapuli, S., Deriel, J. K., Yu, L., and Liuchen, L. Y. (1994) *J. Biol. Chem. 269*, 30195−30199.
3. Wang, J. B., Johnson, P. S., Wu, J. M., Wang, W. F., and Uhl, G. R. (1994) *J. Biol. Chem. 269*, 25966−25969.
4. Chavkin, C., and Goldstein, A. (1981) *Proc. Natl. Acad. Sci. U.S.A. 78*, 6543−6547.
5. Mansour, A., Hoversten, M. T., Taylor, L. P., Watson, S. J., and Akil, H. (1995) *Brain Res. 700*, 89−98.
6. Turcotte, A., Lalonde, J. M., St-Pierre, S., and Lemaire, S. (1984) *Int. J. Pept. Protein Res. 23*, 361−367.
7. Hruby, V. J., and Gehrig, C. A. (1989) *Med. Res. Rev. 9*, 343−401.
8. Paterlini, G., Portoghese, P. S., and Ferguson, D. M. (1997) *J. Med. Chem. 40*, 3254−3262.
9. Martin, W. R., Eades, C. G., Thompson, J. A., Huppler, R. E., and Gilbert, P. E. (1976) *J. Pharmacol. Exp. Ther. 197*, 517−532.
10. Yeagle, P. L., and Albert, A. D. (1998) *Biochem. Soc. Trans. 26*, 520−531.
11. Albert, A. D., and Yeagle, P. L. (2000) *Methods Enzymol. 315*, 107−115.
12. Dyson, H. J., Rance, M., Houghten, R. A., Lerner, R. A., and Wright, P. E. (1988) *J. Mol. Biol. 201*, 161−200.
13. Yeagle, P. L., Alderfer, J. L., and Albert, A. D. (1995) *Nat. Struct. Biol. 2*, 832−834.
14. Yeagle, P. L., Alderfer, J. L., and Albert, A. D. (1995) *Biochemistry 34*, 14621−14625.
15. Yeagle, P. L., Alderfer, J. L., and Albert, A. D. (1997) *Biochemistry 36*, 9649−9654.
16. Yeagle, P. L., Alderfer, J. L., Salloum, A. C., Ali, L., and Albert, A. D. (1997) *Biochemistry 36*, 3864−3869.
17. Katragadda, M., Alderfer, J. L., and Yeagle, P. L. (2000) *Biochim. Biophys. Acta 1466*, 1−6.
18. Mierke, D. F., Royo, M., Pellegrini, M., Sun, H. M., and Chorev, M. (1996) *J. Am. Chem. Soc. 118*, 8998−9004.
19. Pellegrini, M., Royo, M., Chorev, M., and Mierke, D. F. (1996) *Biopolymers 40*, 653−666.
20. Pellegrini, M., and Mierke, D. F. (1997) *J. Med. Chem. 40*, 99−104.
21. Pellegrini, M., Bisello, A., Rosenblatt, M., Chorev, M., and Mierke, D. F. (1998) *Biochemistry 37*, 12737−12743.
22. Piserchio, A., Bisello, A., Rosenblatt, M., Chorev, M., and Mierke, D. F. (2000) *Biochemistry 39*, 8153−8160.
23. Franzoni, L., Nicastro, G., Pertinhez, T. A., Tatò, M., Nakaie, C. R., Paiva, A. C. M., Schreier, S., and Spisni, A. (1997) *J. Biol. Chem. 272*, 9734−9741.
24. Franzoni, L., Nicastro, G., Pertinhez, T. A., Oliveira, E., Nakaie, C. R., Paiva, A. C., Schreier, S., and Spisni, A. (1999) *J. Biol. Chem. 274*, 227−235.
25. Arshava, B., Liu, S. F., Jiang, H., Breslav, M., Becker, J. M., and Naider, F. (1998) *Biopolymers 46*, 343−357.
26. Lauterwein, J., Bösch, C., Brown, L. R., and Wüthrich, K. (1979) *Biochim. Biophys. Acta 556*, 244−264.
27. Vold, R. R., Prosser, R. S., and Deese, A. J. (1997) *J. Biomol. NMR 9*, 329−335.
28. Piotto, M., Saudek, V., and Sklenar, V. (1992) *J. Biomol. NMR 2*, 661−665.
29. Sklenar, V., Piotto, M., Leppik, R., and Saudek, V. (1993) *J. Magn. Reson., Ser. A 102*, 241−245.
30. Havel, T. F. (1991) *Prog. Biophys. Mol. Biol. 56*, 43−78.
31. Guba, W., and Kessler, H. (1994) *J. Phys. Chem. 98*, 23−27.
32. Palczewski, K., Kumasaka, T., Hori, T., Behnke, C. A., Motoshima, H., Fox, B. A., Le Trong, I., Teller, D. C., Okada, T., Stenkamp, R. E., Yamamoto, M., and Miyano, M. (2000) *Science 289*, 739−745.
33. Misra, G. P., and Wong, C. F. (1997) *Proteins: Struct., Funct., Genet. 28*, 344−359.
34. Deber, C. M., and Li, S. C. (1995) *Biopolymers 37*, 295−318.
35. Wüthrich, K. (1986) *NMR of proteins and nucleic acids*, Wiley, New York.
36. Wishart, D. S., Sykes, B. D., and Richards, F. M. (1991) *J. Mol. Biol. 222*, 311−333.
37. Wishart, D. S., Sykes, B. D., and Richards, F. M. (1992) *Biochemistry 31*, 1647−1651.
38. Dyson, H. J., Rance, M., Houghten, R. A., Wright, P. E., and Lerner, R. A. (1988) *J. Mol. Biol. 201*, 201−217.
39. Tessmer, M. R., and Kallick, D. A. (1997) *Biochemistry 36*, 1971−1981.
40. Ferguson, D. M., Kramer, S., Metzger, T. G., Law, P. Y., and Portoghese, P. S. (2000) *J. Med. Chem. 43*, 1251−1252.
41. Schwyzer, R. (1992) *Braz. J. Med. Biol. Res. 25*, 1077−1089.
42. Moroder, L., Romano, R., Guba, W., Mierke, D. F., Kessler, H., Delporte, C., Winand, J., and Christophe, J. (1993) *Biochemistry 32*, 13551−13559.

BI0117955